2019-10

Contribution of speckle noise in near-infrared spectroscopy measurements

Journal of Biomedical Optics

BiomedicalOptics.SPIEDigitalLibrary.org

Contribution of speckle noise in near-infrared spectroscopy measurements

Antonio Ortega-Martinez
Bernhard Zimmermann
Xiaojun Cheng
Xinge Li
Meryem Ayşe Yucel
David A. Boas

SPIE.

Antonio Ortega-Martinez, Bernhard Zimmermann, Xiaojun Cheng, Xinge Li, Meryem Ayşe Yucel, David A. Boas, "Contribution of speckle noise in near-infrared spectroscopy measurements," *J. Biomed. Opt.* **24**(10), 105003 (2019), doi: 10.1117/1.JBO.24.10.105003.

Journal of Biomedical Optics 24(10), 105003 (October 2019)

Contribution of speckle noise in near-infrared spectroscopy measurements

Antonio Ortega-Martinez,* Bernhard Zimmermann, Xiaojun Cheng, Xinge Li, Meryem Ayşe Yucel, and David A. Boas
Boston University, Neurophotonics Center, Biomedical Engineering Department, Boston, Massachusetts, United States

Abstract. Near-infrared spectroscopy (NIRS) is widely used in biomedical optics with applications ranging from basic science, such as in functional neuroimaging, to clinical, as in pulse oximetry. Despite the relatively low absorption of tissue in the near-infrared, there is still a significant amount of optical attenuation produced by the highly scattering nature of tissue. Because of this, designers of NIRS systems have to balance source optical power and source–detector separation to maximize the signal-to-noise ratio (SNR). However, theoretical estimations of SNR neglect the effects of speckle. Speckle manifests as fluctuations of the optical power received at the detector. These fluctuations are caused by interference of the multiple random paths taken by photons in tissue. We present a model for the NIRS SNR that includes the effects of speckle. We performed experimental validations with a NIRS system to show that it agrees with our model. Additionally, we performed computer simulations based on the model to estimate the contribution of speckle noise for different collection areas and source–detector separations. We show that at short source–detector separation, speckle contributes most of the noise when using long coherence length sources. Considering this additional noise is especially important for hybrid applications that use NIRS and speckle contrast simultaneously, such as in diffuse correlation spectroscopy. [DOI: 10.1117/1.JBO.24.10.105003]

Keywords: noise model; speckle; near-infrared spectroscopy; diffuse correlation spectroscopy.

Paper 190267R received Aug. 2, 2019; accepted for publication Oct. 10, 2019; published online Oct. 30, 2019.

1 Introduction

Near-infrared spectroscopy (NIRS) is a technique that exploits the differential absorption of light at different wavelengths to make inferences about chromophores in a sample (typically hemoglobin within biological tissue[1]). In the context of biomedical optics, it is usually performed at wavelengths between 600 and 1000 nm, as those minimize the absorption caused by hemoglobin and water. It has a wide range of applications, including functional brain mapping in the cognitive and psychological sciences,[2,3] sports medicine,[4] and oxygen saturation monitoring.[5]

As the highly scattering nature of tissue prevents light from transmitting through >5 cm of tissue, most NIRS applications are performed in a reflectance geometry.[6,7] In the reflectance geometry, the light source and the detector are placed on the same surface of the sample, usually at a fixed distance. The detector captures a fraction of the light backscattered by the tissue. The backscattered optical power received at a given distance is a function of wavelength and tissue composition, and thus the detected power at different wavelengths can be used to assess biologically relevant information of the tissue. The depth reached by the photons is a function of the source–detector separation as well as the tissue composition (i.e., the scattering and absorption properties of the tissue).[8] For this reason, the source–detector separation needs to be chosen carefully based on the tissue to be studied.

Due to the highly scattering nature of tissue, the detected optical power quickly decreases as the source–detector separation increases. It is not always practical to increase the source power, so in many cases the detectors need to be sensitive enough to detect very small signals. As with any other system, the signal-to-noise ratio (SNR) needs to be larger than one in order to detect a signal. For this reason, characterizing the noise of a system is necessary to understand the limits of the measurable signals, and to be able to design more sensitive systems. Traditionally, the theory of optical measurements takes into account three different sources of noise: (1) light source stability,[9] i.e., the fluctuations in the light intensity; (2) electronic noise, which is independent of the amount of light received, and thus usually conflated with dark noise; and (3) shot noise, which is produced by the statistical nature of the arrival of photons to the detector. As shot noise is a Poisson process, it increases with the square root of the received optical power.[10] When shot noise is the predominant source of noise, a situation known as "shot limited," the SNR grows at most with the square root of the received optical power.

Laser diodes (LDs) are commonly used for fNIRS, as they are easily coupled into optical fibers, and their monochromatic emission makes the spectral analysis of the data more convenient. However, lasers, being coherent light sources, are subject to speckle. Speckle is a phenomenon caused by the interference of light traveling through multiple random paths. Speckle is present in all optical measurements from tissue, as the highly scattering nature of tissue randomizes the photon paths. Speckle manifests as random spatial variations of the received intensity and furthermore dynamics in the scattering sample will generally result in temporal fluctuations in speckle intensity. Although speckle is used in some applications to quantify the sample dynamics[11] (e.g., blood flow), it is undesirable in the context of NIRS. In the extreme case of detection of a single

*Address all correspondence to Antonio Ortega-Martinez, E-mail: aortegam@bu.edu

speckle by a long coherence length laser, the standard deviation of these temporal fluctuations will be equal to the mean intensity of the detected light intensity. These fluctuations, if not sufficiently averaged, will result in excess noise. As a result, any noise model for optical signals should ideally include a component for speckle noise.

In this paper, we propose and validate an extended noise model for NIRS measurements in a reflection geometry that takes into account the effects of speckle. Additionally, we discuss some of the implications of this speckle noise in NIRS systems with the help of simulations.

2 Methods

2.1 *Speckle Theory*

Photons traveling through tissue experience random changes of direction due to scattering. Backscattered photons collected at a detector at a given source–detector separation have an associated probability density function for their path lengths traveled through the scattering sample. These photons interfere with each other and depending on the coherence length of the source light relative to the path length distribution, they might create an observable speckle pattern. The pattern itself is random and fluctuates with a time scale that depends on the dynamics of the scattering particles and the number of scattering events experienced due to the dynamic scattering particles. The electric field associated with the detected optical signal, while randomly fluctuating, has a temporal autocorrelation function modeled as[12] $g_1(\tau) = \exp[-(\tau/\tau_c)^{0.5}]$. In this expression, τ is the time delay and τ_c is the speckle decorrelation time constant. The decorrelation time constant is a function of the speed of the scattering particles in the medium and the distance traveled by the photons in the medium. For photon diffusion through a tissue with blood flow, τ_c is typically given by[13]

$$\tau_c = \frac{1}{6D\mu_s'^2 k_0^2 \alpha \rho^2}. \tag{1}$$

In this expression, D is the effective diffusion coefficient of the red blood cells, μ_s' is the reduced scattering coefficient, k_0 is the wavenumber of the light, α is the probability of scattering being caused by a dynamic scatterer and not by static scattering particles, and ρ is the source–detector separation. If the field autocorrelation is measured, then the decorrelation constant can be found, usually by fitting the data with the exponential model. However, it is usually not practical to measure the field temporal autocorrelation function directly, but instead the intensity temporal autocorrelation function $g_2(\tau)$ can be measured. The Siegert equation describes the relation between both correlations as $g_2(\tau) = 1 + \beta|g_1(\tau)|^2$, where β is an optical constant which depends on the source coherence length, source–detector separation, properties of the scattering medium, and the number of speckles received by the detector.[14] β is usually assumed to be 1, but this is only true when a single-polarized speckle is detected that is generated by a light source with a coherence length longer than the distribution of path lengths of detected light through the scattering sample. For a laser with a random polarization, β is halved. Furthermore, β approaches zero for an incoherent light source such as a light emitting diode (LED).

We define the speckle contrast as $K = \sigma_I/\langle I\rangle$.[15] σ_I is the standard deviation of the speckle intensity, and $\langle I\rangle$ is the mean intensity. In practice, the intensity will be measured by a photodetector with a finite area and a finite integration time T. If the detector captures only one speckle (as in the case of light being delivered to a detector by a single-mode fiber) and $T \gg \tau_c$, the speckle contrast is then reduced because of the temporal averaging of the temporal speckle fluctuations and follows the form $K = \sqrt{\beta\tau_c/T}$.[16] In this case, the noise generated by speckle fluctuations is given by the following expression:

$$\sigma_I = \langle I\rangle\sqrt{\frac{\beta\tau_c}{T}}. \tag{2}$$

Furthermore, if the detector captures M speckles at the same time (such as in the case of light being delivered to the detector by a multimode fiber), the speckle is spatially averaged and the contrast is reduced by the square root of the number of speckles. The speckle noise is then given by

$$\sigma_I = \langle I\rangle\sqrt{\frac{\beta\tau_c}{MT}}. \tag{3}$$

2.2 *Noise Model Including Speckle*

Equation (4) is a noise model for the optical system in watts and is based on existing noise models such as the one seen in Ref. 17, but we modified it to include the contribution of speckle noise:

$$\sigma_{\text{total}} = \sqrt{\left(\frac{\sigma_{i_{\text{dark}}}}{\gamma R_0(\lambda)}\right)^2 + \frac{q_e F}{TR_0(\lambda)}P_D + k_{\text{source}}^2 P_D^2 + \beta\frac{\tau_c}{MT}P_D^2}, \tag{4}$$

where the first term represents the electronic noise converted to optical power at wavelength λ. The second term models the shot noise. The third term models the noise produced by the intensity changes in the optical power of the light source. The fourth term is the speckle noise component given by Eq. (3). $\sigma_{i_{\text{dark}}}$ is the electronic noise expressed in amperes and $R_0(\lambda)$ is the responsivity of the detector at gain $\gamma = 1$. γ is the internal gain of the photodetector. q_e is the charge of an electron, F is the excess noise factor of the photodetector, and P_D is the mean incident optical power on the detector. k_{source} is the coefficient of variation of the light source intensity. In the particular case of the light intensity being captured by an optical fiber, the number of speckles is equal to the number of transmitted modes by the fiber, which is approximated by the expression[18,19] $M = 2(\pi a\text{NA}/\lambda)^2$, with a being the core radius of the fiber and NA its numerical aperture. From Eq. (4), the SNR at full bandwidth for a CW system can be expressed as

$$\text{SNR} = 10\log_{10}\left\{\frac{P_D^2}{\left[\frac{\sigma_{i_{\text{dark}}}}{\gamma R_0(\lambda)}\right]^2 + \frac{q_e F}{TR_0(\lambda)}P_D + k_{\text{source}}^2 P_D^2 + \beta\frac{\tau_c}{MT}P_D^2}\right\}. \tag{5}$$

From Eq. (5), it can be seen that when P_D is large enough, the SNR reaches a limit of $10\log_{10}[MT/(\beta\tau_c)]$, even for a perfectly stable light source. In other words, speckle noise sets a cap to the maximum achievable SNR, and that cap is a function of the light collection geometry, the coherence length of the laser source, the optical characteristics of the sample and the integration time.

2.3 *Experimental Validation of the Model*

We measured the diffuse reflectance of light from a scattering phantom with different incident powers to compare the noise levels with the predictions of our model (Fig. 1). The incident power was controlled with a neutral density filter wheel with 21 positions spanning six orders of magnitude in attenuation. For each position of the filter wheel, light was measured for 30 s with a sampling rate of 25 samples per second. The standard deviation of each time series was calculated to estimate the noise at each incident power level. The detector was an avalanche photodiode integrated into a continuous wave fNIRS system (CW6, TechEn Inc., Massachusetts). The noise was converted to the equivalent optical power by dividing it by the experimentally determined sensitivity of the system (in digital levels per watt).

We used a liquid phantom constructed from silicone thinner (Smooth-On Silicone Thinner, Pennsylvania) as the substrate. Black and white pigments (Smooth-On Silc Pig) were used to give it absorption and scattering properties similar to brain tissue at 830 nm (0.18 and 9.3 cm^{-1}, respectively[20]). The optical characteristics of the phantom at other wavelengths were known through characterization performed with a frequency domain NIRS device (MetaOx, ISS, Champaign, Illinois). As the phantom is liquid, it presented dynamic scattering due to the Brownian motion of the scattering particles. The decorrelation time constant τ_c was 900 μs at the source–detector separation used (diffusion coefficient 0.033 $\mu m^2/s$) as measured with our home-built diffuse correlation spectroscopy (DCS) system.[21] The illumination and detection fibers were set at a fixed distance of $\rho = 10$ mm (center to center) and was chosen to maximize dynamic range of the measurement while keeping the speckle contribution strong. The detector fiber had a core diameter of 200 μm and an NA of 0.22 (SMA step index fiber M25L05 from Thorlabs, New Jersey).

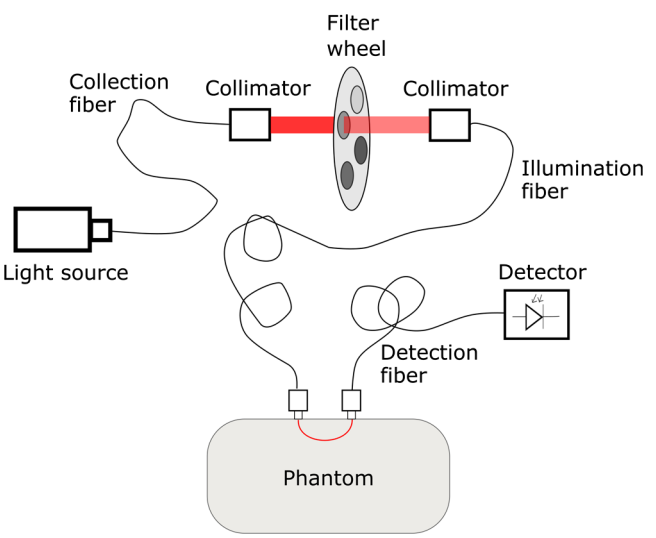

Fig. 1 Experimental setup used to validate the predictions of our noise model. Light is delivered to a phantom with dynamic scatterers through a multimode fiber, and then collected and delivered to the detector by a 200-μm fiber. The light intensity delivered to the phantom is controlled with a neutral density filter wheel.

To show the effect of the coherence of the source on speckle noise, we used three different light sources custom fitted to work with the fNIRS system: an LED, an LD, and a volumetric holographic (VHG) stabilized LD. The LED operated at 850 nm (SMT730D/850D, Marubeni, Tokyo, Japan) and had very short coherence length (expected to be <8 μm). The LD was a Fabry–Perot LD included with the fNIRS system; it operated at 830 nm and has a short coherence length of ~40 μm. The VHG stabilized LD (Thorlabs LP785-SAV50) had a wavelength of 785 nm and a coherence length >10 m. All the light sources were current controlled. The β for each light source was calculated using the theory presented in Ref. 22 and using the parameters of our experimental geometry, the optical properties of phantom, and the coherence length of each light source. The sensitivity of the detector at each wavelength was estimated by measuring the mean signal level on the detector for a known incident optical power. The coefficient of variation of each light source was also characterized with the setup in Fig. 1, by coupling the illumination fiber to the detector fiber instead of using a phantom, eliminating the speckle contribution to noise.

2.4 *Computer Simulation*

We used MATLAB (Mathworks, Natick, Massachusetts) to simulate the noise model described already, which allowed us to visualize how the speckle noise changes for different source–detector separations and fiber core diameters for a typical fNIRS application. This code is freely available at https://github.com/BUNPC/SpeckleNoiseModel, along with code to generate the plots in this paper. Our simulation takes the source–detector separation and fiber core diameter as input parameters and uses them to calculate the incident power on the detector assuming the power of the light source is 5 mW, a typical value for fNIRS systems. The power per unit area incident on the detector as a function of source–detector separation is calculated from the expression found in Ref. 23.

The electronic and shot noise characteristics were modeled for a typical fNIRS system. We assumed that the light is coming from a nonpolarized coherent light source (such as the VHG laser) with $\beta = 0.5$. It was assumed that the source drift was negligible. The NA was fixed to 0.22 for all core diameters. The calculations assumed optical characteristics similar to human tissue, including the speckle decorrelation time constant for measurements on human subjects.[24] All the calculations assume that measurements are made with a full system bandwidth (i.e., the bandwidth is 0.5 T^{-1}). The rest of the simulation parameters are summarized in Table 1, with the exception of the number of modes M, which is a function of the fiber core diameter.

Table 1 Parameters used for the simulation of the noise model. The system characteristics were chosen to match our fNIRS system.

Parameter	$\sigma_{i_{dark}}$	γ	$R_0(\lambda)$	F	T	D	λ	μ_s'	μ_a
Value	3 pA	100	0.55 A/W	7.7	40 ms	2.5 $\mu m^2/s$	785 nm	8 cm^{-1}	0.17 cm^{-1}

3 Results

Figure 2 plots the noise and SNR measured through the dynamic light scattering phantom illuminated by the light sources LED, LD, and VHG (diamonds, squares, and circles, respectively). Predictions of the noise model, calculated with Eq. (4) using the parameters of our system, are shown in solid lines. Phantom measurements were consistent with the prediction of the noise model. Figure 2(a) displays the noise (converted to equivalent optical power by dividing by the sensitivity at the appropriate wavelength) for each incident power. Additionally, it shows the predominant noise component at high power for each light source (dashed lines): shot noise for the LED, source fluctuations for the LD, and speckle noise for the VHG. Figure 2(b) plots the SNR. We can see that noise levels stay relatively constant at low incident optical power and then start increasing after the optical noise starts dominating the electronic noise. At high optical power, the slope for the noise is 0.5 for the LED and 1 for the VHG and LD. The coefficient of variation of the VHG and LD sources, i.e., k_{source} from Eq. (4), had a similar value of 4.6×10^{-4} but was one order of magnitude lower for the LED.

In Fig. 3, we present the results of our simulation for the speckle noise fraction as a function of source–detector separation and fiber diameter using as a contour plots. The color represents the percentage of the total noise variance produced by speckle at each fiber diameter and source–detector separation.

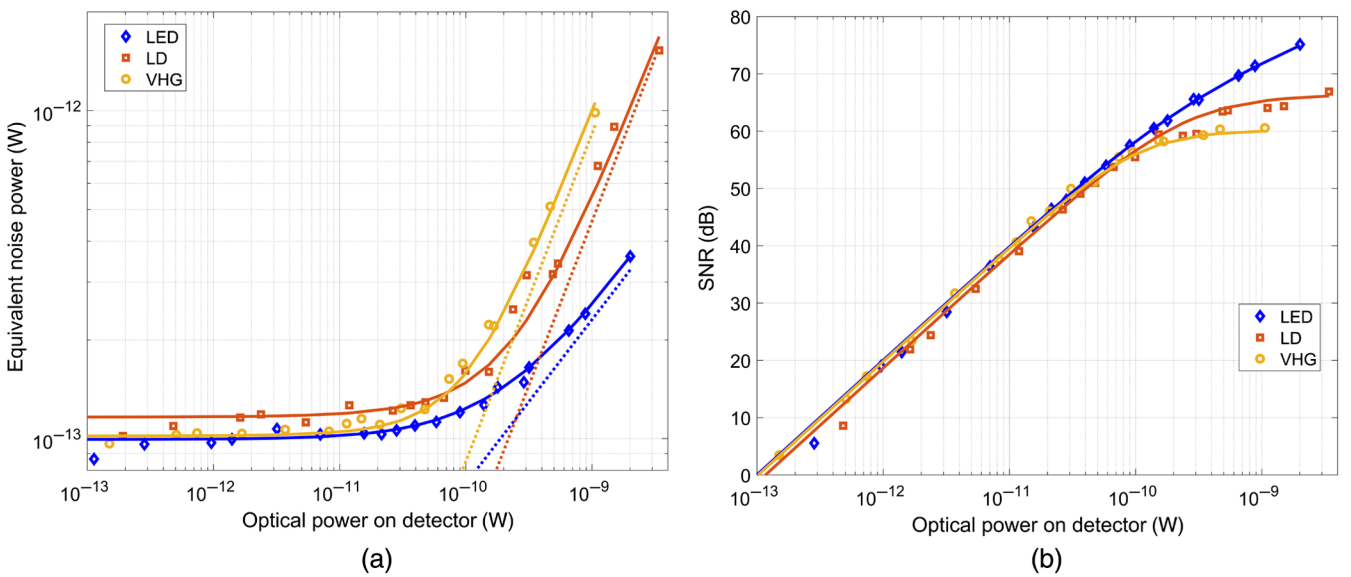

Fig. 2 Results of the validation experiments (diamonds, squares, and circles) for the three different light sources (LED, LD, and VHG, respectively), as well as what is expected from the model (solid lines). (a) The absolute amount of noise at each incident optical power; the dashed lines show the contribution of the predominant noise component for each light source. (b) The SNR in decibels.

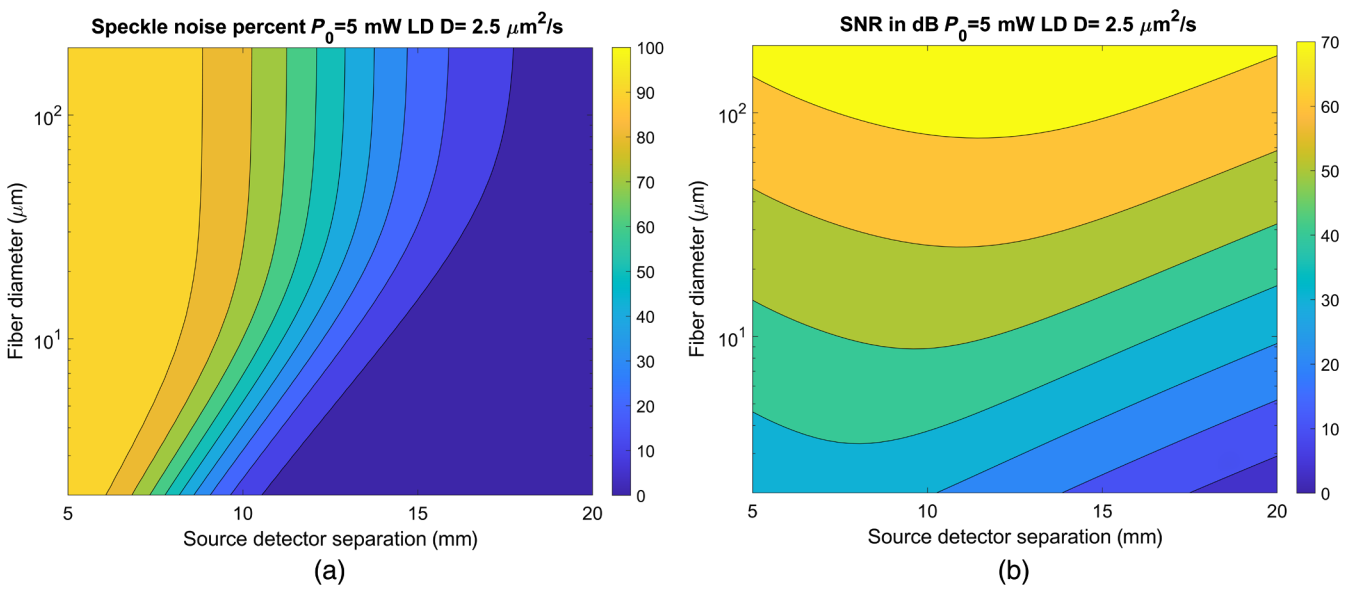

Fig. 3 (a) Speckle noise percentage and (b) SNR in decibels as a function of fiber core diameter and source–detector separation, as calculated using our model for the VHG (high coherence) laser.

We plot fiber diameter along the vertical axis which is associated with an increasing amount of received optical power as larger fiber diameters collect more light. Increasing source–detector separation along the horizontal axis is associated with an increasing number of scattering events which decreases τ_c and decreasing optical power. For short source–detector separations, speckle noise dominates, even for large fiber diameters. For long source–detector separations, other noise sources dominate: electronic noise on the lower right quadrant, as optical power is very small, and shot noise on the upper right corner as optical power increases with fiber diameter. Figure 3(b) shows the SNR in decibel for the same conditions as in Fig. 3(a).

4 Discussion

Figure 2 shows the expected noise and SNR behavior for the three light sources. When the optical power is small, the electronic noise of the system dominates, and the noise level is relatively constant. Above a certain optical power threshold (around 10^{-10} W), optical noise becomes important and the measured noise starts increasing as a function of optical power. As the shot noise grows with the square root of the optical power, the slope in the shot noise limited regime is 0.5 on a log–log scale. However, as speckle and source noise grow linearly with optical power, there will be a threshold where they will dominate shot noise and electronic noise. We can observe this behavior in Fig. 2(a). Although the slope of the noise of the LED source is 0.5, the LD and VHG curves are growing with a slope closer to one due to speckle and source fluctuations. The effect of this slope in the SNR can be observed in Fig. 2(b). The three SNR curves grow linearly with optical power while the noise is electronic limited. The LED curve keeps growing even at high optical powers but becomes shot noise limited, growing only with a slope of 0.5. The LD and VHG curves become flat and stop growing, as predicted by Eq. (5), due to the effects of speckle noise and source power fluctuations.

In Fig. 2(a), we can also see that the predictions made with the theory fit the experimental results well. Using our model, we can quantify what percentage of the noise is caused by speckle. At high optical powers, speckle produces 5% of the total noise for the LD, but 73% for the VHG. This is consistent with the large difference in their coherence lengths (estimated to be 40 μm for the LD and 10 m for the VHG).

From Fig. 3, we can see that speckle noise dominates at short source–detector separations for optical and dynamic properties typical of measurements on human brain for a long coherence length light source. Although Fig. 3 shows the result for a very specific case, some patterns are easy to predict from the model. As speckle noise is a function of the received optical power, increasing the power of the light source while keeping all other parameters constant will increase the percentage of speckle noise, moving the contour of Fig. 3(a) to the right. Similarly, increasing τ_c, as is associated with slower dynamics and thus less temporal averaging, increases the speckle noise, moving the contour to the right. Although we used a diffusion coefficient D of 2.5 $\mu m^2/s$ for this simulation, we have experimentally observed values on humans as small as 1 $\mu m^2/s$, which corresponds with roughly a 60% increase in the absolute amount of speckle noise. On the other hand, a light source with a shorter coherence length will produce less speckle and thus shift the contour to the left.

From Eq. (3), we see that the amount of speckle noise is directly proportional to the mean optical power on the detector and inversely proportional to the square root of the number of modes detected, i.e., $\sigma_{\text{speckle}} \propto P_D/\sqrt{M}$. However, both the number of modes and the power on the detector are proportional to the square of the detector fiber radius $P_D \propto a^2$ and $M \propto a^2$. This means that for a collection fiber geometry, the absolute amount of speckle noise grows linearly with fiber core radius.

Figure 3(b) provides some complementary information to Fig. 3(a) by showing the SNR for the different combinations of fiber diameter and source–detector separation. Due to speckle noise at short separations reducing SNR, the SNR maxima for a given fiber diameter happens at an "intermediate" source–detector separation. When the separation is small, speckle reduces the SNR; when the separation is large, low received optical power limits the SNR because of a higher shot and electronic noise contribution. The precise location of the maxima moves to the right as fiber diameter increases.

Although speckle represents a problem in the context of NIRS measurements, there are techniques such as DCS which rely on speckle contrast to make quantitative assessments of tissue dynamics, in particular blood flow. For DCS, speckle is not considered noise but it is instead the source of the signal, and thus it is desirable to maximize it. The usual strategy is using single-mode fibers to increase speckle averaging. However, from Fig. 3(a), we can see that speckle dominates at short detection separation regardless of fiber diameter. On the other hand, hypothetical hybrid techniques combining NIRS and DCS will have to take into account the effects of speckle noise for the NIRS measurement. On these systems, highly coherent light sources are desirable to increase speckle contrast and thus improve the SNR of the measurements of the sample dynamics. However, at the same time, this speckle will decrease the SNR of the NIRS measurement. Based on this, choosing a laser with an appropriate coherence length will be important to maximize the SNR of both measurements.

5 Conclusions

The theoretical framework presented in this paper provides important guidance in designing NIRS devices to optimize the SNR. As suggested by the theory and backed up by the experimental data, speckle can produce a significant amount of excess noise when making NIRS measurements using highly coherent lasers. This is a noise factor that has generally not been considered in NIRS measurements. The contribution of speckle noise easily dominates shot noise at small source–detector separations, placing an upper limit on the maximum achievable SNR, even for highly stable light sources. This means that for samples with dynamic scattering, increasing the power of the light source produces diminishing results after some point. Furthermore, as the upper limit is specific to a given geometry and sample, the only convenient way to increase it is by having a larger integration time, which ultimately reduces the maximum achievable response time of the system. On the other hand, the dominance of speckle at short source–detector separations means that applications relying on speckle, such as DCS, can potentially relax some design requirements for specific geometries by allowing for the use of larger diameter fibers.

Disclosures

The authors declare no potential conflicts of interest.

Acknowledgments

This work was funded by a research contract under Facebook's Sponsored Academic Research Agreement. In addition, this work received funding from NIH Nos. R24-NS104096 and R01-EB025145.

References

1. M. Ferrari and V. Quaresima, "A brief review on the history of human functional near-infrared spectroscopy (fNIRS) development and fields of application," *Neuroimage* **63**(2), 921–935 (2012).
2. L. Ferreri et al., "The promise of near-infrared spectroscopy (NIRS) for psychological research: a brief review," *Annee Psychol.* **114**(3), 537–569 (2014).
3. S. Cutini, S. B. Moro, and S. Bisconti, "Review: functional near infrared optical imaging in cognitive neuroscience: an introductory review," *J. Near Infrared Spectrosc.* **20**(1), 75–92 (2012).
4. T. Hamaoka et al., "The use of muscle near-infrared spectroscopy in sport, health and medical sciences: recent developments," *Philos. Trans. R. Soc. A* **369**(1955), 4591–4604 (2011).
5. A. Pellicer and M. D. C. Bravo, "Near-infrared spectroscopy: a methodology-focused review," *Semin. Fetal Neonatal Med.* **16**(1), 42–49 (2011).
6. C. Balas, "Review of biomedical optical imaging—a powerful, non-invasive, non-ionizing technology for improving in vivo diagnosis," *Meas. Sci. Technol.* **20**(10), 104020 (2009).
7. H. Dehghani et al., "Multiwavelength three-dimensional near-infrared tomography of the breast: initial simulation, phantom, and clinical results," *Appl. Opt.* **42**(1), 135–145 (2003).
8. G. E. Strangman, Z. Li, and Q. Zhang, "Depth sensitivity and source-detector separations for near infrared spectroscopy based on the Colin27 brain template," *PLoS One* **8**(8), e66319 (2013).
9. T. Sanvito et al., "A method for characterizing the stability of light sources," *Opt. Express* **21**(21), 24630–24635 (2013).
10. M. Xiao, L.-A. Wu, and H. J. Kimble, "Precision measurement beyond the shot-noise limit," *Phys. Rev. Lett.* **59**(3), 278–281 (1987).
11. D. A. Boas and A. K. Dunn, "Laser speckle contrast imaging in biomedical optics," *J. Biomed. Opt.* **15**(1), 011109 (2010).
12. M. A. Davis et al., "Sensitivity of laser speckle contrast imaging to flow perturbations in the cortex," *Biomed. Opt. Express* **7**(3), 759–775 (2016).
13. D. A. Boas et al., "Establishing the diffuse correlation spectroscopy signal relationship with blood flow," *Neurophotonics* **3**(3), 031412 (2016).
14. T. Bellini et al., "Effects of finite laser coherence in quasielastic multiple scattering," *Phys. Rev. A* **44**(8), 5215–5223 (1991).
15. J. D. Briers and S. Webster, "Laser speckle contrast analysis (LASCA): a nonscanning, full-field technique for monitoring capillary blood flow," *J. Biomed. Opt.* **1**(2), 174–179 (1996).
16. D. D. Postnov et al., "Dynamic laser speckle imaging," *bioRxiv* **2**, 626515 (2019).
17. F. Xu, M.-A. Khalighi, and S. Bourennane, "Impact of different noise sources on the performance of PIN- and APD-based FSO receivers," in *Proc. 11th Int. Conf. Telecommun.*, pp. 211–218 (2011).
18. P. E. Green, *Fiber Optic Networks*, Illustrate, Prentice Hall, Hawthorne, New York (1993).
19. A. Efimov, "Different measures of speckle and coherence at the output of a multimode optical fiber," *J. Opt. Soc. Am. A* **36**(1), 1–11 (2019).
20. J. D. Johansson, "Spectroscopic method for determination of the absorption coefficient in brain tissue," *J. Biomed. Opt.* **15**(5), 057005 (2010).
21. D. Tamborini et al., "Development and characterization of a multidistance and multiwavelength diffuse correlation spectroscopy system," *Neurophotonics* **5**(1), 011015 (2017).
22. X. Cheng et al., "Time domain diffuse correlation spectroscopy: modeling the effects of laser coherence length and instrument response function," *Opt. Lett.* **43**(12), 2756–2759 (2018).
23. T. J. Farrell, M. S. Patterson, and B. Wilson, "A diffusion theory model of spatially resolved, steady-state diffuse reflectance for the noninvasive determination of tissue optical properties in vivo," *Med. Phys.* **19**(4), 879–888 (1992).
24. S. A. Carp et al., "Due to intravascular multiple sequential scattering, diffuse correlation spectroscopy of tissue primarily measures relative red blood cell motion within vessels," *Biomed. Opt. Express* **2**(7), 2047–2054 (2011).

Antonio Ortega-Martinez is currently a biomedical engineering PhD candidate at the BOAS Lab at Boston University. He has a bachelor's degree in electrical engineering and his master's degree in optics. Currently, he is researching diffuse correlation spectroscopy (DCS), wearable devices for functional near infrared spectroscopy (fNIRS) and signal processing techniques for brain computer interfaces (BCI). His main interest lies in translating optical techniques from the lab to practical and/or commercial applications.

Bernhard Zimmermann is a postdoctoral researcher at the Boston University Neurophotonics Center. He received his MSc degree from ETH Zurich in electrical engineering and his PhD from MIT in electrical engineering and computer science. His main research interests are the development of novel instrumentation for diffuse optical techniques such as functional near-infrared spectroscopy (fNIRS) and diffuse correlation spectroscopy (DCS).

Xiaojun Cheng has studied wave scattering problems inside random media for her PhD thesis at the City University of New York. She is now a postdoctoral fellow working on physiological models based on real microvascular networks, as well as wave interference effects in all kinds of optical systems.

Xinge Li is a first-year doctoral student in the Clinical Psychology Program at the University of Houston. He earned a BS degree in psychology in 2012 and his MS degree in applied psychology in 2015. After graduating, he worked as a research fellow for three years at Massachusetts General Hospital and Boston University, focusing on studying brain functions using optical neuroimaging methods. Her primary research interests are in using mutimodality neuroimaging methods to predict potential protective and risk factors regarding normal and aberrant early neurodevelopment.

Meryem Ayşe Yucel is an assistant in Biomedical Engineering at Massachusetts General Hospital, and an instructor at Harvard Medical School, Department of Radiology. Currently, she is a research assistant professor in the Department of Biomedical Engineering at Boston University, her primary focus is on functional near-infrared spectroscopy and translating the method to clinical applications and disseminating its use in basic neuroscience research. She has expertise in mathematical modeling of biological systems and functional brain imaging (fNIRS, fMRI, and EEG).

David A. Boas is the director of the Boston University Neurophotonics Center, and is a professor of biomedical engineering. He has degrees from the Rensselear Polytechnic Institute and the University of Pennsylvania. He is the founding president of the Society for Functional Near Infrared Spectroscopy and founding Editor-in-Chief of the journal *Neurophotonics* published by SPIE. He was awarded the Britton Chance Award in Biomedical Optics in 2016 for his development of several novel, high-impact biomedical optical technologies in the neurosciences, as well as following through with impactful application studies, and fostering the widespread adoption of these technologies.